β1,4-*N*-Acetylgalactosaminyltransferase III Enhances Malignant Phenotypes of Colon Cancer Cells

John Huang,[1,5] Jin-Tung Liang,[1] Hsiu-Chin Huang,[6] Tang-Long Shen,[3] Hsiao-Yu Chen,[4] Neng-Yu Lin,[4] Mei-leng Che,[4] Wei-Chou Lin,[2] and Min-Chuan Huang[4]

Departments of [1]Surgery and [2]Pathology, National Taiwan University Hospital; [3]Department of Plant Pathology and Microbiology, National Taiwan University; and [4]Institute of Anatomy and Cell Biology and [5]Graduate Institute of Clinical Medicine, National Taiwan University College of Medicine, Taipei, Taiwan; and [6]Animal Technology Institute Taiwan, Miaoli, Taiwan

Abstract

The enzyme β1,4-*N*-acetylgalactosaminyltransferase III (β4GalNAc-T3) exhibits *in vitro* activity of synthesizing *N,N′*-diacetyllactosediamine, GalNAcβ1,4GlcNAc. Here, we investigate the expression of *β4GalNAc-T3* in primary colon tumors and the effects of its overexpression on HCT116 colon cancer cells. Real-time reverse transcription-PCR showed that the expression of *β4GalNAc-T3* was up-regulated in 72.5% (*n* = 40) of primary colon tumors compared with their normal counterparts. *β4GalNAc-T3* overexpression resulted in enhanced cell-extracellular matrix adhesion, migration, anchorage-independent cell growth, and invasion of colon cancer cells. Moreover, *β4GalNAc-T3* overexpression increased tumor growth and metastasis and decreased survival of tumor-bearing nude mice. *β4GalNAc-T3* overexpression showed increased tyrosine phosphorylation of focal adhesion kinase and paxillin Y118 as well as increased extracellular signal–regulated kinase phosphorylation. These results suggest that up-regulation of *β4GalNAc-T3* may play a critical role in promoting tumor malignancy and that integrin and mitogen-activated protein kinase signaling pathways could be involved in the underlying mechanism. (Mol Cancer Res 2007;5(6):543–52)

Introduction

Altered carbohydrate structures on cell surfaces are prominent features of cancer cells. Alterations in glycosylation include differential expression of naturally occurring glycans and neo-expression of glycans normally restricted to embryonic tissues (1). Tumor-associated carbohydrate epitopes commonly found in various cancers include T, Tn, Globo H, Lewis y, sialyl Lewis x, sialyl Lewis a, and polysialic acid (2-6). Changes in expression levels of glycosyltransferases can lead to modifications in the core and terminal structures of N-linked and O-linked glycoconjugates as well as glycolipids. However, differential expressions of glycosyltransferases in tumors and their effects on cancer cell phenotypes are still not well understood.

Carbohydrate changes on cell surfaces play important roles in cell-cell and cell-extracellular matrix (ECM) interactions. Integrins, surface glycoprotein receptors for ECM, have been suggested to regulate cell-ECM adhesion, cell migration, invasion, and cell survival (7). Several reports show that alterations of integrin glycosylation affect cancer cell migration and invasion. ST6Gal-I has been shown to sialylate β_1 integrins and up-regulate colon cancer cell migration (8). GnT-III introduces bisecting GlcNAc into integrin $\alpha_5\beta_1$ and down-regulates cell adhesion and migration (9). Aberrant N-glycosylation of β_1 integrin induced by GnT-V causes reduced $\alpha_5\beta_1$ integrin clustering and stimulates cell migration (10). Furthermore, overexpression of ST6GalNAc I causes a significant change in the O-glycosylation of integrin β_1 chain and leads to alterations of cell morphology and behavior (11). Recently, we found that C2GnT-M overexpression decreases colon cancer cell growth and tyrosine phosphorylation of paxillin, which is an important downstream signaling molecule of integrins (12). In addition, β3Gn-T6 was found to decrease core 1 structure and suppress metastatic potential of colon carcinoma cells through an unclear mechanism (13). These studies suggest that glycosyltransferases can regulate cancer cell behavior through alterations of integrin glycosylation or through other mechanisms which remain to be identified.

β4GalNAc-T3 has been shown to be significantly expressed in the gastrointestinal tract (14). In addition, the recombinant enzyme can transfer GalNAc to GlcNAc and form *N,N′*-diacetyllactosediamine (GalNAcβ1,4GlcNAc) in both *N*- and *O*-glycans by an *in vitro* enzyme activity assay. However, the biological and pathologic functions of *β4GalNAc-T3* in the gastrointestinal tract remain unclear.

In the present study, we show that *β4GalNAc-T3* is frequently up-regulated in primary colon tumors when compared with their normal mucosa. To elucidate the effects of *β4GalNAc-T3* on colon cancer cell behavior, *β4GalNAc-T3* was overexpressed in HCT116 cells. Cell adhesion, migration, invasion, and anchorage-independent cell growth *in vitro*, as

Received 12/20/06; revised 2/20/07; accepted 2/26/07.
Grant support: National Health Research Institute grant NHRI-EX95-9410BC (M-C. Huang), National Taiwan University Hospital grant NTUH-94M13 (J. Huang), and Frontier and Innovative Research Program, National Taiwan University grant 95R0101 (M-C. Huang).
The costs of publication of this article were defrayed in part by the payment of page charges. This article must therefore be hereby marked *advertisement* in accordance with 18 U.S.C. Section 1734 solely to indicate this fact.
Note: J. Huang and J-T. Liang contributed equally to this work.
Requests for reprints: Min-Chuan Huang, Institute of Anatomy and Cell Biology, National Taiwan University College of Medicine, No. 1, Sec. 1 Jen-Ai Road, Taipei 100, Taiwan. Phone: 886-2-2312-3456, ext. 8177; Fax: 886-2-2391-5292. E-mail: mchuang@ntu.edu.tw

doi:10.1158/1541-7786.MCR-06-0431

well as tumor growth and metastasis *in vivo*, were significantly enhanced by *β4GalNAc-T3* overexpression. The increase in malignant phenotypes was associated with activation of focal adhesion kinase (FAK) and extracellular signal–regulated kinase (ERK) mitogen-activated protein kinase (MAPK) signalings. These results suggest that up-regulation of *β4GalNAc-T3* may contribute to the malignant behavior of colon cancer cells.

Results

β4GalNAc-T3 *Is Up-Regulated in Primary Colorectal Tumors*

To determine whether *β4GalNAc-T3* expression is altered in colon cancer, real-time reverse transcription-PCR (RT-PCR) was done. PCR products were sequenced and confirmed to be correct. Results from real-time RT-PCR showed that *β4GalNAc-T3* mRNA expression can be easily detected in normal colon mucosa from 92.5% (37 of 40) of colon cancer patients (Fig. 1A). Interestingly, we found that 72.5% (29 of 40) of colon tumors exhibited up-regulation of *β4GalNAc-T3* expression compared with their normal counterparts (Fig. 1A). Among which, 15 (37.5%) patients showed that *β4GalNAc-T3* expression in tumor tissues was 1- to 10-fold higher than that in their paired normal tissues (Fig. 1B). In addition, 14 (35%) patients showed >10-fold increase in *β4GalNAc-T3* expression in colon tumors compared with their normal tissues. In contrast, only 8 (20%) patients showed down-regulation. These results suggest that *β4GalNAc-T3* expression is frequently up-regulated in primary colon tumors.

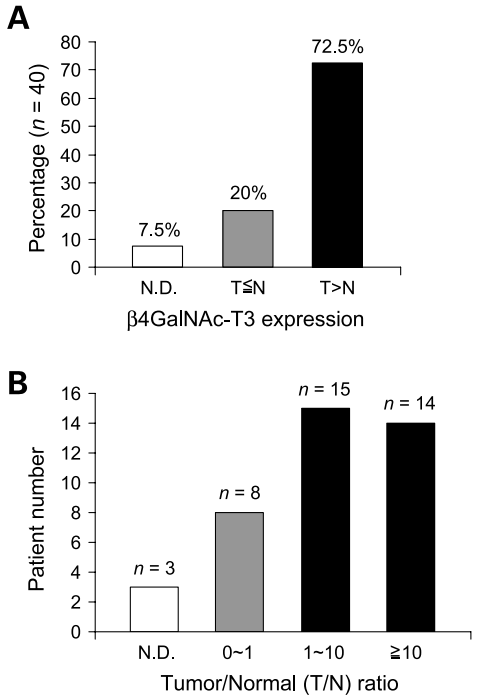

FIGURE 1. Expression of *β4GalNAc-T3* in primary colon tumors by real-time RT-PCR. **A.** *β4GalNAc-T3* is frequently up-regulated in colon tumors compared with their normal counterparts. Expression levels of *β4GalNAc-T3* in paired colon tissues from 40 patients (n = 40) were analyzed by real-time RT-PCR. The percentages of the three groups were shown. N.D., not detectable; T, tumor; N, normal. **B.** Of the 40 patients tested, numbers of patients with different tumor/normal (*T/N*) ratios of *β4GalNAc-T3* expression are shown. n, patient number.

β4GalNAc-T3 *Enhances Cell Adhesion to ECM*

To investigate the effects of *β4GalNAc-T3* expression on colon cancer cells, HCT116 cells were stably transfected with *β4GalNAc-T3*/pcDNA3.1 plasmids (a gift from Dr. Hisashi Narimatsu) or mock transfected with pcDNA3.1 control plasmids. *β4GalNAc-T3* overexpression in HCT116 was confirmed by real-time RT-PCR and Western blotting as well as flow cytometry with a panel of lectins (data not shown). As shown in Fig. 2A, we observed that *β4GalNAc-T3* transfectants (clones 3 and 5) exhibited significant morphologic changes on cell culture plates. As shown in Fig. 2B, 59% to 61.8% of *β4GalNAc-T3* stable transfectants exhibited spreading morphology after seeding cells for 6 h. However, only 20.9% of mock transfectants spread. The spreading of mock transfectants was observed mostly after seeding for 24 h; this is similar to HCT116 parental cells. These data suggest that *β4GalNAc-T3* overexpression may enhance cell adhesion of colon cancer cells.

Cell-ECM interactions play essential roles in cancer cell migration and invasion. To examine the effect of *β4GalNAc-T3* expression on cell adhesion to ECM, we analyzed cell adhesiveness to collagen IV, fibronectin, or laminin under serum-free conditions. As shown in Fig. 2C and D, both *β4GalNAc-T3* transfectants showed a significant increase in adhesion to collagen IV, fibronectin, and laminin in a dose-dependent manner compared with mock transfectants. In addition, we found that *β4GalNAc-T3* transfectants adhered stronger to cell culture plates without ECM than did mock transfectants (data not shown). These results suggest that *β4GalNAc-T3* overexpression enhances colon cancer cell adhesion to collagen IV, fibronectin, and laminin.

β4GalNAc-T3 *Increases Cell Migration*

To examine whether *β4GalNAc-T3* overexpression can regulate cell migration, a monolayer wound healing assay was done. We found that the migration of *β4GalNAc-T3* transfectants was significantly faster than that of mock transfectants (Fig. 3A). The average migration rates of mock and *β4GalNAc-T3* transfectants were 3.3 and 9.6 to 12.5 μm/h, respectively (Fig. 3B). In addition, we observed that *β4GalNAc-T3* overexpression enhanced HCT116 cell migration by Boyden chamber cell migration assays (data not shown). These stimulatory effects of *β4GalNAc-T3* on cell migration were not due to increased rates of cell proliferation because we could not detect significant changes in growth rate over a 16-h period among the two transfectants. These results suggest that *β4GalNAc-T3* expression significantly increases the motility of colon cancer cells.

β4GalNAc-T3 *Overexpression Increases Cell Invasion*

Next, we examined the effect of *β4GalNAc-T3* on cell invasion by a Matrigel invasion assay, which mimics active transmigration of cancer cells across a reconstituted basement membrane. Invading cell numbers of *β4GalNAc-T3* transfectants

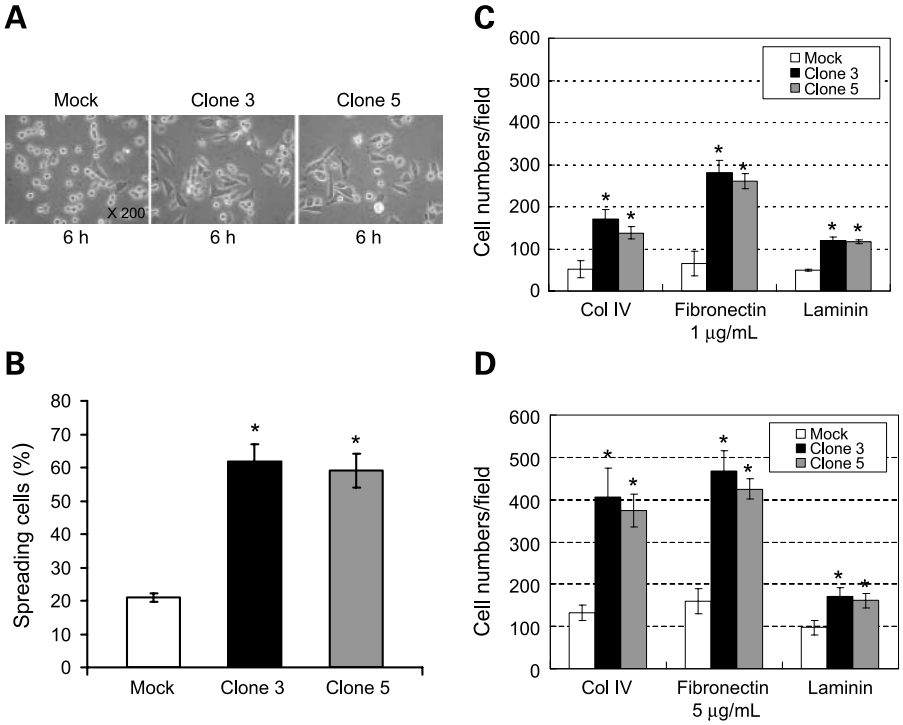

FIGURE 2. *β4GalNAc-T3* increases cell adhesion. **A** and **B.** *β4GalNAc-T3* increases cell spreading on substratum. Mock and β4GalNAc-T3 transfectants of HCT116 cells were seeded onto six-well plates. After 6 h, cells were photographed and shown in **A**. Magnification is indicated on the bottom right corner. **B.** Spreading cells of mock (*open column*) and *β4GalNAc-T3* transfectants (*black* and *gray columns*) were calculated at five different fields. Columns, mean from three independent experiments; bars, SD. *, $P < 0.01$. **C** and **D.** *β4GalNAc-T3* increases cell adhesion to ECM. Cells were plated onto 96-well plates precoated with 1 μg/mL (**C**) or 5 μg/mL (**D**) of human collagen IV (*Col IV*), human fibronectin (*FN*), and murine Engelbreth-Holm-Swarm laminin (*LM*). Mock (*open columns*) and *β4GalNAc-T3* (*black* and *gray columns*) stable transfectants (2×10^4) were seeded onto each well of 96-well plates and incubated at 37°C for 30 min. Nonspecific binding cells were carefully removed and specific adherent cells were counted under a phase-contrast microscope. Three independent experiments were analyzed. *, $P < 0.01$, compared with mock transfectants.

were 51 to 64 per field (Fig. 4A and B). However, only 9 invaded cells were observed for mock transfectants. To further confirm the effect of *β4GalNAc-T3* on cell invasion, *β4GalNAc-T3* expression of clone 3 stable transfectants was knocked down by small interfering RNA (siRNA). We found that *β4GalNAc-T3* siRNA, but not control siRNA, significantly suppressed *β4GalNAc-T3* expression after 48-h transfection (Fig. 4C). In addition, the invasive ability of *β4GalNAc-T3*-knockdown cells was also significantly decreased compared with cells knocked down by control siRNA (Fig. 4D). Given that, these results suggest that *β4GalNAc-T3* can markedly promote colon cancer cell invasion.

Effects of β4GalNAc-T3 *Expression on Anchorage-Dependent and Anchorage-Independent Cell Growth*

To know whether *β4GalNAc-T3* overexpression can affect anchorage-dependent cell growth, cell viability was analyzed by trypan blue exclusion assays. We found that *β4GalNAc-T3* transfectants did not affect cell growth significantly, observed from day 1 to day 6 (Fig. 5A).

Next, we analyzed the effect of *β4GalNAc-T3* overexpression on anchorage-independent cell growth by colony formation assays in soft agar. As shown in Fig. 5B, the colony number of *β4GalNAc-T3* transfectants was 2.1- to 2.5-fold more than the mock transfectants, suggesting that *β4GalNAc-T3* overexpression can increase the colony-forming ability of HCT116 cells.

β4GalNAc-T3 *Enhances Tumor Growth in Nude Mice*

To test whether *β4GalNAc-T3* overexpression can alter tumor growth *in vivo*, we inoculated BALB/c (*nu/nu*) mice subcutaneously with mock or *β4GalNAc-T3* stable transfectants. At day 20 after inoculation, mice were sacrificed and tumors were excised for analyses. The *β4GalNAc-T3* tumors showed an average wet weight of 1.64 to 1.97 g compared with 0.20 g in mock tumors ($n = 5$ tumors each; $P < 0.001$; Fig. 6A), representing an 8- to 10-fold increase in tumor mass. The size of *β4GalNAc-T3* tumors was homogeneous and much larger than mock tumors (Fig. 6B). Macroscopically, hypervascularity was observed on the surface of all *β4GalNAc-T3* tumors (Fig. 6B). In contrast, blood vessels were rarely present on mock tumors. Microscopically, vascularization of *β4GalNAc-T3* tumors was dramatically increased compared with poorly vascularized mock tumors (data not shown). These results suggest active angiogenesis in *β4GalNAc-T3* tumors. In addition, we found that all *β4GalNAc-T3* tumors showed severe invasion into not only adjacent skeletal muscles but also the peritoneum. In sharp contrast, mock tumors showed intact capsules without local invasion. These results suggest that *β4GalNAc-T3* is a potent stimulator of tumor growth *in vivo*.

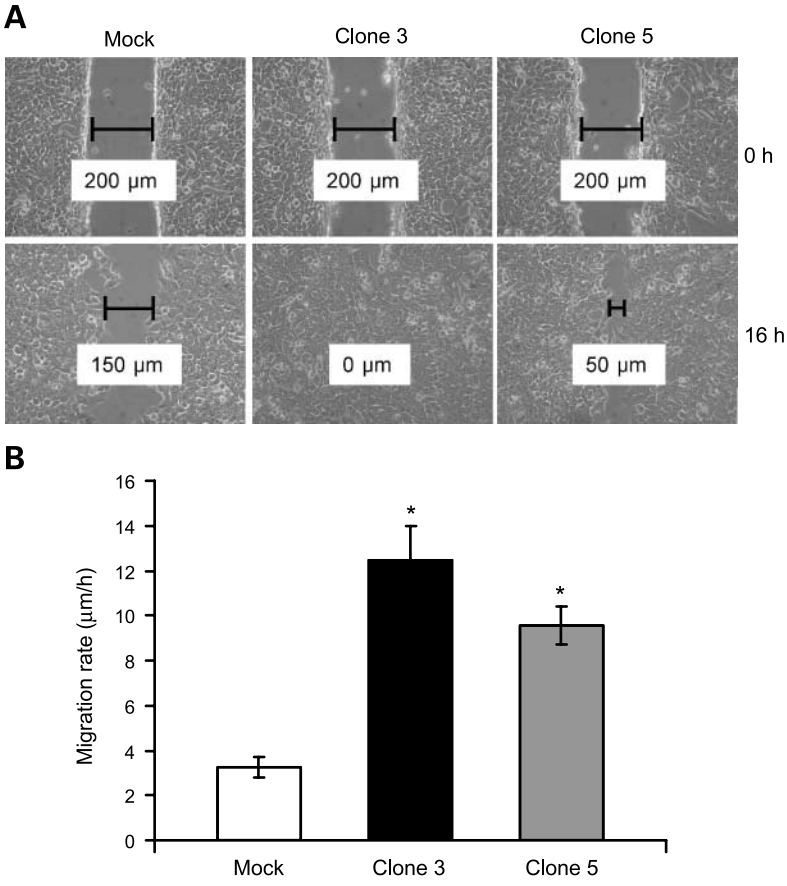

FIGURE 3. *β4GalNAc-T3* enhances cell migration. **A.** *β4GalNAc-T3* overexpression enhances cell migration analyzed by wound healing assays. Confluent cells were scraped with a 250-μL tip for 200 μm and observed for 16 h. Representative images are shown at the indicated times. Lines, clear regions of scraped areas; the distance (μm) is as indicated. Magnification, ×200. **B.** Migration rate of mock (*open column*) and *β4GalNAc-T3* (*black* and *gray columns*) transfectants is presented as migration distance (μm)/time (h). Three independent experiments were analyzed. *, $P < 0.01$, compared with mock transfectants.

β4GalNAc-T3 *Decreases Survival and Increases Tumor Metastasis in Nude Mice*

Next, we assessed the survival rate of nude mice intraperitoneally injected with *β4GalNAc-T3* trasfectants. All nude mice with *β4GalNAc-T3* transfectants ($n = 4$ for each clone) died by day 50 after injection (Fig. 6C). In addition to large amount of ascites in peritoneum, tumor nodules were observed in the kidney, liver, spleen, and intestine in these mice (Fig. 6D). In sharp contrast, 100% of control nude mice ($n = 5$) injected with mock transfectants were still survived at 50 days ($P = 0.001$).

For tumor metastasis analysis, nude mice were injected with mock transfectants (control, $n = 5$) or *β4GalNAc-T3* transfectants ($n = 5$ for each clone) through tail vein. We found that severe lung metastasis of colon cancer cells was observed in mice injected with *β4GalNAc-T3* transfectants (tumor nodules, $n = 17$-22) but not mock transfectants (tumor nodules, $n = 3$; Fig. 6E). In addition, the metastasis was confirmed by H&E staining of lungs (Fig. 6F). These findings suggest that *β4GalNAc-T3* overexpression can increase tumor metastasis and decrease survival.

Effects of β4GalNAc-T3 *Expression on Tyrosine Phosphorylation of FAK and Paxillin as well as MAPK Phosphorylation*

Our data showed that *β4GalNAc-T3* transfectants significantly enhanced cell-ECM adhesion, migration, and invasion. Because integrin-ECM interactions have been shown to play key roles in regulating these phenotypic changes, we investigated whether integrin-mediated signalings could be regulated by *β4GalNAc-T3* overexpression. Cells were replated on fibronectin-coated culture dishes under serum-free conditions and tyrosine phosphorylation of FAK and paxillin, key signaling molecules downstream of integrins, was analyzed by Western blot. As shown in Fig. 7A, there was no significant difference in FAK expression between *β4GalNAc-T3* and mock transfectants. However, tyrosine phosphorylation levels of FAK in *β4GalNAc-T3* stable transfectants were significantly increased compared with mock transfectants, as detected by both monoclonal antibodies 4G10 and PY20. We also found that FAK pY397 and pY576 were increased in these cells (Fig. 7B). In addition, an increase in paxillin pY118 in *β4GalNAc-T3* transfectants was observed, with total paxillin levels unchanged (Fig. 7C). Interestingly, paxillin pY31 was decreased in *β4GalNAc-T3* transfectants. Only results from clone 3 were shown. Similar results were also observed in clone 5 (data not shown).

Because cell migration and malignant cell survival are associated with MAPK activation, effects of *β4GalNAc-T3* overexpression on MAPK phosphorylation were analyzed. We found that overexpression of *β4GalNAc-T3* significantly increased ERK (Fig. 7D) but not c-jun NH_2-terminal kinase and p38 (data not shown) MAPK phosphorylation. However, expression levels of total ERK remain unchanged. Only results

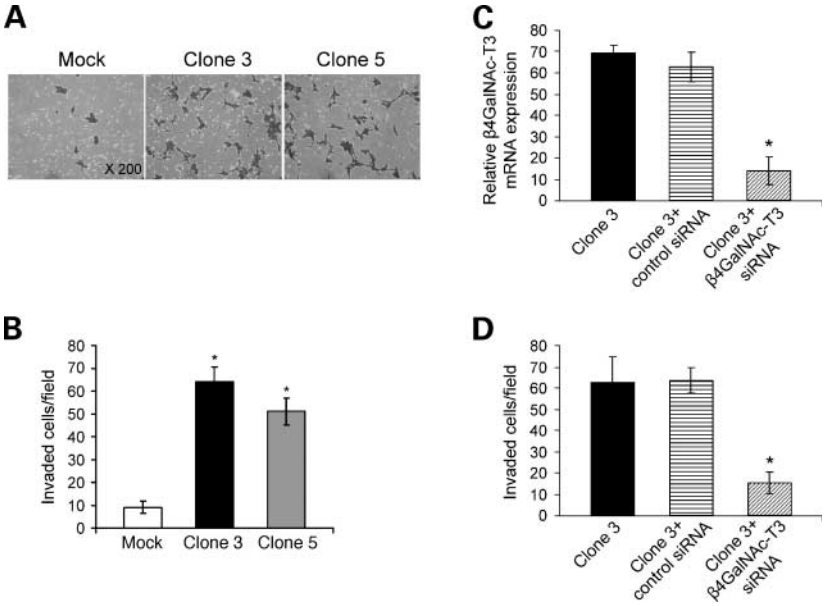

FIGURE 4. *β4GalNAc-T3* increases colon cancer cell invasion. **A** and **B.** *β4GalNAc-T3* overexpression promotes cell invasiveness analyzed by Matrigel invasion assays. Mock or *β4GalNAc-T3* transfectants (2×10^5) were seeded in each chamber and cultured for 48 h. Invaded cells were fixed with 100% methanol and stained with 0.5% crystal violet (*top*). **A.** Representative images. **B.** The invaded cells of mock (*open column*) and *β4GalNAc-T3* (*black* and *gray columns*) stable transfectants from five fields were counted under a phase-contrast microscope. Columns, mean from three independent experiments; bars, S.D. *, $P < 0.01$, compared with mock transfectants. **C.** *β4GalNAc-T3* expression in clone 3 stable transfectants is knocked down by *β4GalNAc-T3* siRNA but not control siRNA. The relative *β4GalNAc-T3* mRNA levels normalized to *β-actin* in cells after 48-h transfection of siRNA were analyzed by real-time RT-PCR. Clone 3, clone 3 of *β4GalNAc-T3* stable transfectants; Clone 3 + control siRNA, clone 3 cells transfected with control siRNA; Clone 3 + *β4GalNAc-T3* siRNA, clone 3 cells transfected with *β4GalNAc-T3* siRNA. *, $P < 0.01$, compared with clone 3 knocked down by control siRNA. **D.** Invasive ability of *β4GalNAc-T3*-knockdown cells is reduced. Cells were seeded into Matrigel invasion chambers for 48 h. The invaded cell numbers were counted under a microscope. *, $P < 0.01$, compared with clone 3 knocked down by control siRNA.

from clone 3 were shown. Similar results were also observed in clone 5 (data not shown). These results suggest that overexpression of *β4GalNAc-T3* is capable of activating FAK and ERK MAPK activity.

Discussion

β4GalNAc-T3 is highly expressed in the gastrointestinal tract and testes and exhibits an *in vitro* activity of synthesizing *N,N′*-diacetyllactosediamine, GalNAcβ1,4GlcNAc (14). In the

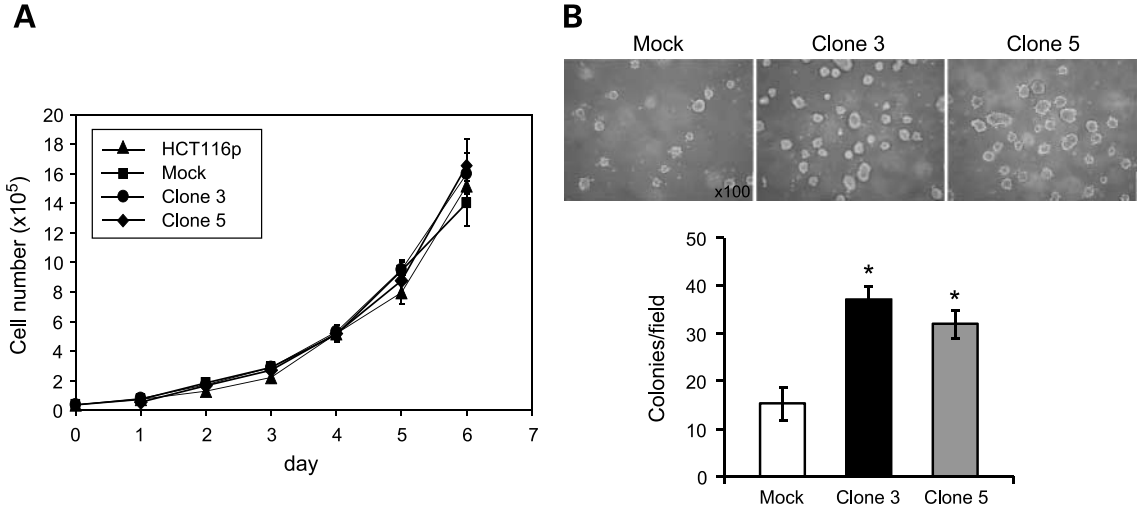

FIGURE 5. Effects of β4GalNAc-T3 expression on anchorage-dependent and anchorage-independent cell growth. **A.** Anchorage-dependent cell growth is not affected by β4GalNAc-T3. Viable cells were observed for 6 d and analyzed by trypan blue exclusion assays, which were quantified from three independent experiments. **B.** β4GalNAc-T3 enhances anchorage-independent cell growth of HCT116 cells in soft agar. Mock (*open column*) and β4GalNAc-T3 (*black* and *gray columns*) were seeded into soft agar for 14 d. Colony numbers (colony size >50 μm) were counted under a microscope after crystal violet staining. Magnification, ×100. Columns, mean from three independent experiments; bars, SD. *, $P < 0.01$, compared with mock transfectants.

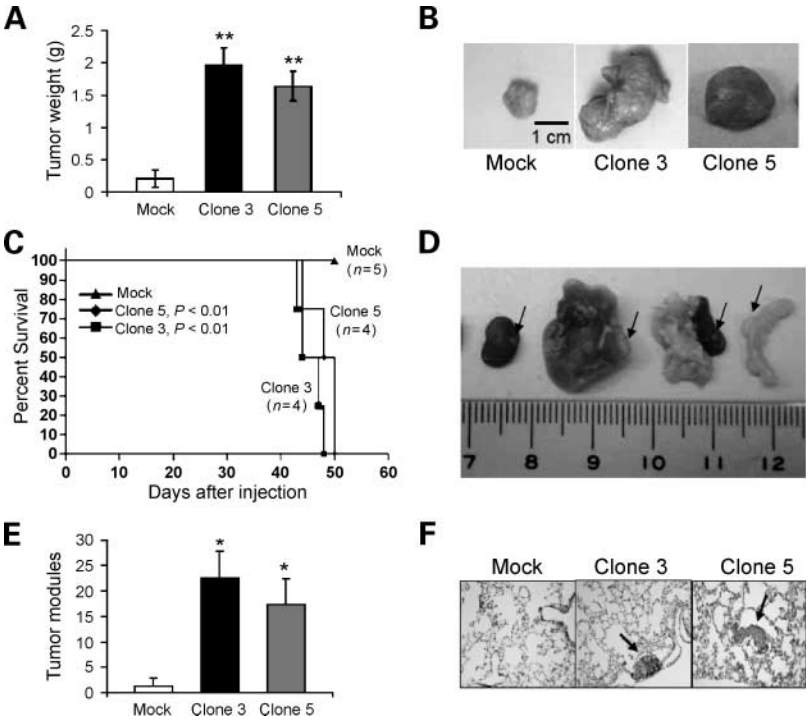

FIGURE 6. *β4GalNAc-T3* promotes tumor growth and metastasis and decreases survival in nude mice. **A** and **B.** *β4GalNAc-T3* promotes tumor growth *in vivo*. Mock or β4GalNAc-T3 stable transfectants (5×10^6) were injected subcutaneously. into nude mice ($n = 5$ per group). Mice were sacrificed 20 d after injection. **A.** The excised mock (*open column*) or *β4GalNAc-T3* (*black* and *gray columns*) tumors were weighed. Columns, mean; bars, SD. **, $P < 0.001$, compared with mock transfectants. **B.** Tumor size was dramatically increased in mice xenografted with β4GalNAc-T3 stable transfectants. Representative images of tumors; bar, 1 cm. **C** and **D.** *β4GalNAc-T3* decreases survival of nude mice. **C.** For survival analysis, nude mice were intraperitoneally injected with mock or *β4GalNAc-T3* transfectants as indicated. The survival rate was calculated by the Kaplan-Meier method. The survival rate was significantly lower in mice with *β4GalNAc-T3* tumors ($P = 0.001$; $n = 4$ for each clone) compared with that in the control mice with mock tumors ($n = 5$). **D.** Tumor metastasis was observed in various organs of mice with β4GalNAc-T3 tumors, including kidney, liver, pancreas, and intestine. **E** and **F.** *β4GalNAc-T3* promotes tumor metastasis in nude mice. **E.** Average number of tumor nodules in lungs of nude mice. **F.** Histologic analysis of lung metastasis of mock and *β4GalNAc-T3* transfectants. Arrows, tumor nodules. Magnification, ×100.

present study, we found that *β4GalNAc-T3* is up-regulated in 72.5% colon tumors compared with their normal counterparts. Overexpression of *β4GalNAc-T3* increases malignant phenotypes of colon cancer cells both *in vitro* and *in vivo*. These findings suggest that *β4GalNAc-T3* may play a crucial role in promoting malignant behaviors of colon cancer.

The ability to migrate and invade through ECM proteins into surrounding tissues is essential for tumor progression and

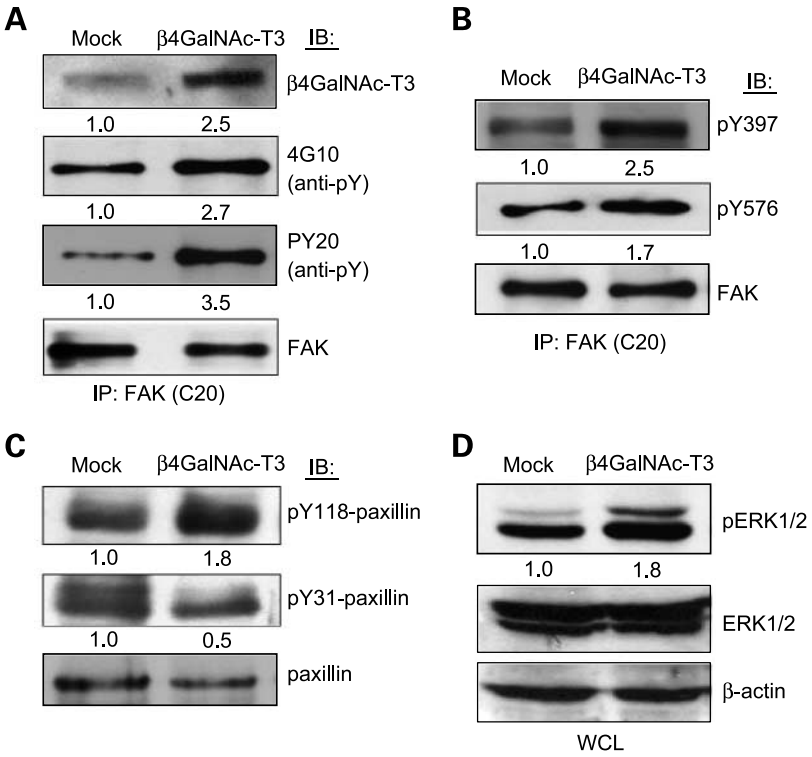

FIGURE 7. Effects of β4GalNAc-T3 on signal transduction. **A.** β4GalNAc-T3 increases tyrosine phosphorylation of FAK. To show β4GalNAc-T3 overexpression in HCT116 stable transfectants, equal amount of cell extracts was immunoblotted with anti–β4GalNAc-T3 antibody. For FAK analysis, cell extracts were immunoprecipitated (*IP*) with anti-FAK (C20) antibody and then immunoblotted (*IB*) with C20 (anti-FAK), 4G10 (anti-pY), or PY20 (anti-pY) monoclonal antibody, as indicated. The band intensity was quantified by ImageQuant 5.1 and normalized to total FAK or β-actin (not shown) levels. **B.** β4GalNAc-T3 increases tyrosine phosphorylation of FAK Y397 and Y576. Cell extracts were immunoprecipitated with anti-FAK (C20) antibody and then Western blotted with anti-FAK pY397, pY576 or anti-FAK (C20), as indicated. Signal amounts were quantified and normalized to total FAK. **C.** β4GalNAc-T3 increases tyrosine phosphorylation of paxillin Y118 but decreases tyrosine phosphorylation of paxillin Y31. Cell extracts were immunoblotted with anti-paxillin pY118, pY31 or anti-paxillin, as indicated. The band intensity was quantified and normalized to total paxillin levels. **D.** β4GalNAc-T3 increases phosphorylation of ERK MAPK. Total ERK1/2 and pERK1/2 were detected by immunoblotting of whole-cell lysate (*WCL*) with anti–total ERK and anti–phospho-ERK, respectively. β-Actin was used as a control. The band intensity of pERK1/2 was quantified and normalized to total ERK1/2 levels. Representative of at least three independent experiments.

metastasis. Here, we found that *β4GalNAc-T3* overexpression significantly enhances cell adhesion, migration, and invasion. Integrins are important surface receptors to mediate these cell-ECM interactions, and integrin-mediated signalings through FAK and paxillin have been suggested to play important roles in malignant behavior of cancer cells (7, 15-19). Recently, changes in expression levels of glycosyltransferases have been found to alter integrin signaling and thereby regulate cell behavior. For example, GnT-III overexpression inhibits cell spreading and migration on fibronectin and decreases FAK phosphorylation (9). ST6Gal-I overexpression results in increased association of β_1 integrin and talin, indicating that integrin signaling is activated (8). Interestingly, we found that both integrin-mediated autophosphorylation of FAK at Y397 and Src family–dependent tyrosine phosphorylation of FAK at Y576 were increased in *β4GalNAc-T3* transfectants. Y397 is the major FAK autophosphorylation site and its phosphorylation is critical for subsequent binding of Src family kinases. Src-mediated transphosphorylation of Y576 within the kinase domain maximizes the catalytic activity of FAK (20). In addition, we found that tyrosine phosphorylation of FAK-Src substrate paxillin at Tyr^{118} was also increased. These results strongly suggest that *β4GalNAc-T3* is capable of inducing integrin-mediated FAK signaling pathways. Notably, we found that phosphorylation levels of paxillin Y31 were decreased in *β4GalNAc-T3* transfectants, although cell-ECM adhesion and cell migration were increased, suggesting that pY118, but not pY31, plays the predominant role in enhancing HCT116 cell migration. To our knowledge, this is the first report showing that paxillin pY31 is decreased whereas pY118 is increased. Several reports show that both Y31 and Y118 are the primary FAK-Src targets and then proteins with SH2 domains bind to pY31 and pY118, which in turn regulate cell motility (21). However, the functional difference between pY31 and pY118 is still unclear. Our findings suggest that tyrosine phosphorylation of Y31 and Y118 can be regulated separately, transmitting appropriate signals for cells to respond to particular stimuli. It will be of great interest to investigate the differential signaling roles of pY31 and pY118 by the use of the *β4GalNAc-T3* transfectants.

MAPK signalings have been suggested to play crucial roles in cell migration (22-24) as well as tumor progression and invasion (25, 26). For example, ERK regulates cell movement by phosphorylating myosin light chain kinase, calpain, FAK, or paxillin, which have been shown to modulate adhesion dynamics (23, 27-29). Furthermore, MAPKs have been shown to regulate cell invasion by modulating the proteolytic enzymes that degrade the basement membrane (25). In agreement with these findings, our data showed that enhanced cell adhesion, migration, and invasion of *β4GalNAc-T3* transfectants correlated with increased ERK phosphorylation. These results suggest that increased ERK MAPK signalings could play a critical role in the increased migration and invasion of colon cancer cells induced by *β4GalNAc-T3* overexpression.

Many reports show that glycosyltransferases can directly modify carbohydrates on cell-surface receptors or cell-adhesion molecules and then regulate signal transduction and cell behavior. GnT-V, GnT-III, ST6GalNAc I, and ST6Gal-I were found to directly modify carbohydrate structures on β1-integrin and affect integrin activity (8-11). These changes in N-glycosylation (8, 30) or O-glycosylation (11) of β1-integrin lead to altered cell morphology and behavior. Furthermore, GnT-III was found to modify carbohydrates on epidermal growth factor receptor and inhibit ERK-mediated neurite outgrowth in PC12 cells (31). In addition, GnT-III can also modify the glycosylation of cadherin and down-regulate tyrosine phosphorylation of β-catenin in mouse melanoma, human colon cancer, and human hepatoma cell lines (32). Interestingly, *β4GalNAc-T3* has been shown to efficiently modify both *N*- and *O*-glycans decorated with GlcNAc *in vitro* (14). We therefore speculate that *β4GalNAc-T3* may directly glycosylate *N*- or/and *O*-glycans of integrins or other surface molecules such as the epidermal growth factor receptor family. The changes in glycosylation of these surface receptors then modulate integrin and MAPK signaling pathways and, in turn, regulate cell phenotyes.

In the present study, *β4GalNAc-T3* overexpression dramatically increased tumor size. However, cell proliferation *in vitro* was not significantly changed. These data suggest that tumor cell-host interactions, such as angiogenesis, may play a crucial role in tumor growth. Indeed, hypervascularity was found in *β4GalNAc-T3* tumors, but not mock tumors, suggesting that the increase in tumor growth induced by *β4GalNAc-T3 in vivo* could be at least, in part, resulted from angiogenesis.

Taken together, we show important roles of *β4GalNAc-T3* in colon cancer cells. We present evidence that *β4GalNAc-T3* overexpression significantly promotes malignant behaviors of colon cancer cell both *in vitro* and *in vivo*. These phenotypic changes induced by *β4GalNAc-T3* are associated with enhanced integrin and MAPK signalings. The present study provides a new insight into the molecular mechanism by which glycosyltransferases may play a key role in regulating tumor malignancy.

Materials and Methods

Cell Culture and Transfection

Colon cancer cell line HCT116 from American Type Culture Collection was maintained with DMEM (JRH Biosciences) containing 10% fetal bovine serum (FBS; PAA Laboratories GmbH) in a humidified tissue culture incubator at 37°C in a 5% CO_2 atmosphere. For stable transfection, 4 μg of *β4GalNAc-T3*/pcDNA3.1 (ref. 14; a kind gift from Dr. Hisashi Narimatsu) or pcDNA3.1/myc-His (InVitrogen, Life Technologies, Inc.) were transfected into 5×10^5 HCT116 cells by use of Lipofectamine 2000 (InVitrogen, Life Technologies). After 24 h of transfection, the cells were trypsinized and plated onto three 100-mm dishes with 10% FBS-DMEM containing 800 μg/mL of G418 (Calbiochem). After 2 weeks of selection, G418-resistant clones were isolated and transferred to 24-well plates. The expression levels of *β4GalNAc-T3* were analyzed by real-time RT-PCR and Western blotting with anti–*β4GalNAc-T3* polyclonal antibodies. Several pcDNA3.1/myc-His–transfected clones (HCT116/Mock) and *β4GalNAc-T3*–positive clones including clones 3 and 5 were selected for experiments.

Real-time RT-PCR

Total cellular RNA was isolated from cells grown to 70% confluence by use of the Trizol reagent (Invitrogen, Life

Technologies) according to the manufacturer's protocols as previously described (33). For cDNA synthesis, 2 μg of total RNA were used as template in a 25-μL reverse transcription reaction. Matched RNA pairs of colorectal cancer patients were used for real-time RT-PCR. All the clinical materials were obtained from patients at National Taiwan University Hospital after informed consent was given. For *β-actin* detection, sense and antisense primers were 5′-GCTCGTC-GTCGACAACGGCT-3′ and 5′-AAACATGATCTGGGTCAT-CTTCT-3′, respectively, generating a 326-bp fragment. For detection of *β4GalNAc-T3*, sense and antisense primers were 5′-CTACAGCGCATTGTGAACGT-3′ and 5′-TGGTTCTTCA-CAGGCACGAC-3′, respectively, generating a 320-bp fragment.

For real-time PCR reactions, quantitative PCR System Mx3000P (Stratagene) was used according to the manufacturer's protocol. Briefly, reaction was done in a 25-μL volume with 2 μL of cDNA, 400 nmol/L each of sense and antisense primers, and 12.5 μL of Brilliant SYBR Green QPCR Master Mix (Stratagene). PCRs were incubated for 15 min at 95°C followed by 40 amplification cycles with 30-s denaturation at 95°C, 50-s annealing at 54°C, and 30-s extension at 72°C. Samples were analyzed in triplicate, and product purity was checked through dissociation curves at the end of real-time PCR cycles. Relative quantity of gene expression normalized to β-actin was analyzed with MxPro Software (Stratagene).

Cell Spreading and Morphology

The same numbers of cells were seeded onto 60-mm culture plates (Falcon). After 6 h, cells were photographed with a digital camera (Nikon COOLPIX5400). Spreading cells were calculated at three different fields and results are presented as means ± SD from three independent experiments.

Cell Adhesion Assay

Cell adhesion assays were done according to published protocols with slight modifications (12). Ninety-six-well plates were coated with bovine serum albumin (BSA) control, human collagen IV (Sigma), human fibronectin (Sigma), or murine laminin (Sigma) at concentrations of 1 or 5 μg/mL in PBS at 37°C for 4 h, and then blocked with 1% bovine serum albumin at 37°C for 2 h. Cells were trypsinized, washed with DMEM, and recovered in DMEM at 37°C for 40 min. Mock and *β4GalNAc-T3* stable transfectants (2×10^4) in 100-μL serum-free DMEM per well were allowed to attach for 30 min at 37°C in a humidified 5% CO_2 incubator. Attached cells from four wells were counted manually under an inverted microscope. The number of specific adherent cells indicates the difference between the number of cells binding to ECM-coated wells and the number of cells binding to bovine serum albumin–coated wells. All data are expressed as means ± SD from three independent experiments.

Wound Healing Assay

Cells were seeded onto 12-well culture dishes and grown until confluence in DMEM containing 10% FBS. The monolayer was scratched with a 250-μL yellow tip. Migration of cells to the wounded area was observed under an inverted microscope and pictures were taken directly at the time of scratching and after scratching for 16 h. Measurements were taken from five individual microscopic fields in each experiment, and the data from three experiments are presented.

Matrigel Invasion Assay

Cell invasion assays were done in BioCoat Matrigel Invasion Chambers (Becton Dickinson) according to the manufacturer's protocols. Briefly, 500-μL DMEM containing 10% FBS was loaded in the lower part of the chamber and 3×10^5 cells in 500-μL serum-free DMEM were seeded onto the upper part. Cells were allowed to invade the Matrigel for 48 h in a humidified tissue culture incubator at 37°C, 5% CO_2 atmosphere. Noninvading cells on the upper surface of the membrane were removed from the chamber, and the invading cells on the lower surface of the membrane were fixed with 100% methanol and stained with 0.5% crystal violet (Sigma). The numbers of invading cells in each well were counted under a phase-contrast microscope. The means ± SD were calculated from the numbers of invading cells from three independent experiments under a microscope.

Cell Growth Analysis

Mock and *β4GalNAc-T3* stable transfectants (4×10^4) were seeded onto six-well plates. Six wells were plated for each time point, which was taken at 24-h intervals for 6 days. Viable cells were determined for each time point with a hemocytometer by trypan blue exclusion. Three independent experiments were done and the count results were used for plotting the relative growth rate with SD.

Anchorage-Independent Growth in Soft Agar

Cells (1×10^4) in 0.3% Bactoagar (Sigma) in DMEM supplemented with 10% FBS were overlaid on a base of 0.6% Bactoagar in DMEM supplemented with 10% FBS in six-well plates. Cells were incubated at 37°C, 5% CO_2 atmosphere. Triplicate wells for each cell line and three independent experiments were done. The numbers of colonies with diameter >50 μm were counted at day 14.

siRNA Knockdown of β4GalNAc-T3 Expression

SMARTpool siRNA oligonucleotides against *β4GalNAc-T3* and siCONTROL Nontargeting siRNA were synthesized by Dharmacon Research, Inc. For knockdown of *β4GalNAc-T3*, cells were transfected with siRNA using Lipofectamine 2000 (InVitrogen) with a final concentration of 100 nmol siRNA. The cells were incubated for 4 h and then serum-free DMEM was replaced with complete DMEM (10% FBS). After 48-h incubation, cells were harvested for analysis. The knockdown of *β4GalNAc-T3* expression was confirmed by real-time RT-PCR.

Western Blot

Cells were resuspended in serum-free DMEM and replated onto fibronectin-coated dishes for 16 h. Equal amounts of cell

lysate were electrophoresed on SDS-PAGE and transferred to a nitrocellulose membrane. Membranes were incubated with anti–phospho-Tyr (PY20 from Transduction Laboratories and 4G10 from Upstate Biotechnology), anti-FAK pY397, pY576 polyclonal antibody (Biosources), anti-FAK polyclonal antibody (C-20, Santa Cruz Biotechnology), anti-paxillin pY118, pY31 (BD Transduction Lab), anti-paxillin polyclonal antibody (BD Transduction Lab), anti–β-actin monoclonal antibody (BD Biosciences, CA), mouse anti–phospho-MAPK monoclonal antibodies and rabbit anti-ERK1/2 polyclonal antibody (Cell Signaling Technology), or anti–β4GalNAc-T3 polyclonal antibody, which was generated by immunizing rabbits with keyhole limpet hemocyanin conjugated with a synthetic *β4GalNAc-T3* peptide: ARMLEGRQTPASTLEQ-DATD. The membrane was incubated with horseradish peroxidase–conjugated antirabbit or antimouse immunoglobulin G (Santa Cruz Biotechnology). Signals were visualized with enhanced chemiluminescence reagents (Amersham Biosciences) and images were quantified with ImageQuant 5.1 (Amersham Biosciences).

Tumor Growth, Tumor Metastasis, and Survival Rate in Nude Mice

For tumor growth analysis, 6-week-old female BALB/c nude mice were injected subcutaneously with 5×10^6 of HCT116/Mock transfectants ($n = 5$), *β4GalNAc-T3* transfectants clone 3 ($n = 5$), or *β4GalNAc-T3* transfectants clone 5 ($n = 5$). At day 20 after injection, tumors in each group were excised for analyses.

For tumor metastasis analysis, 6-week-old female BALB/c nude mice were injected with 2×10^6 of HCT116/Mock transfectants (control, $n = 5$), *β4GalNAc-T3* transfectants clone 3 ($n = 5$), or *β4GalNAc-T3* transfectants clone 5 ($n = 5$) through tail vein. The tumors in the lungs were excised after injection for 50 days and fixed with 4% paraformaldehyde for H&E staining.

For survival assays, 6-week-old female BALB/c nude mice were intraperitoneally injected with 2×10^6 of HCT116/Mock transfectants (control, $n = 5$), *β4GalNAc-T3* transfectants clone 3 ($n = 4$), or *β4GalNAc-T3* transfectants clone 5 ($n = 4$). All mice were monitored twice a week for body weight and other abnormalities for 50 days. Once life-threatening symptoms became markedly manifest, the mice were sacrificed. The organs, including kidneys, lungs, pancreas, intestines, and liver, were analyzed. Survival analysis was done using the Kaplan-Meier method.

Statistical Analysis

Student's t test was used for statistical analyses. Data are presented as means ± SD. Survival analysis was done using the Kaplan-Meier method with a log-rank test for comparison. $P < 0.05$ was considered significant.

Acknowledgments

We thank Dr. Hisashi Narimatsu (National Institute of Advanced Industrial Science and Technology, Japan) for *β4GalNAc-T3*/pcDNA3.1 plasmids and Dr. Chuan-Ching Lai (Institute of Anatomy and Cell Biology, National Taiwan University College of Medicine) and Chia-Ying Tsai and Yu-Ming Huang (National Taiwan University School of Medicine) for their technical support.

References

1. Dube D, Bertozzi C. Glycans in cancer and inflammation—potential for therapeutics and diagnostics. Nat Rev Drug Discov 2005;4:477–88.

2. Hakomori S. Glycosylation defining cancer malignancy: new wine in an old bottle. Proc Natl Acad Sci U S A 2002;99:10231–3.

3. Sell S. Cancer-associated carbohydrates identified by monoclonal antibodies. Hum Pathol 1990;21:1003–19.

4. Hakomori S, Zhang Y. Glycosphingolipid antigens and cancer therapy. Chem Biol 1997;4:97–104.

5. Taylor-Papadimitriou J, Epenetos A. Exploiting altered glycosylation patterns in cancer: progress and challenges in diagnosis and therapy. Trends Biotechnol 1994;12:227–33.

6. Tanaka F, Otake Y, Nakagawa T, et al. Expression of polysialic acid and STX, a human polysialyltransferase, is correlated with tumor progression in non-small cell lung cancer. Cancer Res 2000;60:3072–80.

7. Guo W, Giancotti F. Integrin signalling during tumour progression. Nat Rev Mol Cell Biol 2004;5:816–26.

8. Seales E, Jurado G, Brunson B, Wakefield J, Frost A, Bellis S. Hypersialylation of β_1 integrins, observed in colon adenocarcinoma, may contribute to cancer progression by up-regulating cell motility. Cancer Res 2005; 65:4645–52.

9. Isaji T, Gu J, Nishiuchi R, et al. Introduction of bisecting GlcNAc into integrin $\alpha_5\beta_1$ reduces ligand binding and down-regulates cell adhesion and cell migration. J Biol Chem 2004;279:19747–54.

10. Guo H, Lee I, Kamar M, Akiyama S, Pierce M. Aberrant N-glycosylation of β_1 integrin causes reduced $\alpha_5\beta_1$ integrin clustering and stimulates cell migration. Cancer Res 2002;62:6837–45.

11. Clement M, Rocher J, Loirand G, Le Pendu J. Expression of sialyl-Tn epitopes on β_1 integrin alters epithelial cell phenotype, proliferation and haptotaxis. J Cell Sci 2004;117:5059–69.

12. Huang M, Chen H, Huang H, et al. C2GnT-M is down-regulated in colorectal cancer and its re-expression causes growth inhibition of colon cancer cells. Oncogene 2006;25:3267–76.

13. Iwai T, Kudo T, Kawamoto R, et al. Core 3 synthase is down-regulated in colon carcinoma and profoundly suppresses the metastatic potential of carcinoma cells. Proc Natl Acad Sci U S A 2005;102:4572–7.

14. Sato T, Gotoh M, Kiyohara K, et al. Molecular cloning and characterization of a novel human β1,4-*N*-acetylgalactosaminyltransferase, β4GalNAc-T3, responsible for the synthesis of *N,N′*-diacetyllactosediamine, galNAc β1-4GlcNAc. J Biol Chem 2003;278:47534–44.

15. Playford M, Schaller M. The interplay between Src and integrins in normal and tumor biology. Oncogene 2004;23:7928–46.

16. Gabarra-Niecko V, Schaller M, Dunty J. FAK regulates biological processes important for the pathogenesis of cancer. Cancer Metastasis Rev 2003;22:359–74.

17. Schlaepfer D, Mitra S, Ilic D. Control of motile and invasive cell phenotypes by focal adhesion kinase. Biochim Biophys Acta 2004;1692:77–102.

18. McLean G, Carragher N, Avizienyte E, Evans J, Brunton V, Frame M. The role of focal-adhesion kinase in cancer—a new therapeutic opportunity. Nat Rev Cancer 2005;5:505–15.

19. Owens L, Xu L, Craven R, et al. Overexpression of the focal adhesion kinase (p125FAK) in invasive human tumors. Cancer Res 1995;55:2752–5.

20. Mitra S, Hanson D, Schlaepfer D. Focal adhesion kinase: in command and control of cell motility. Nat Rev Mol Cell Biol 2005;6:56–68.

21. Brown M, Turner C. Paxillin: adapting to change. Physiol Rev 2004;84: 1315–39.

22. Anand-Apte B, Zetter B, Viswanathan A, et al. Platelet-derived growth factor and fibronectin-stimulated migration are differentially regulated by the Rac and extracellular signal-regulated kinase pathways. J Biol Chem 1997;272:30688–92.

23. Klemke R, Cai S, Giannini A, Gallagher P, de Lanerolle P, Cheresh D. Regulation of cell motility by mitogen-activated protein kinase. J Cell Biol 1997; 137:481–92.

24. Huang C, Jacobson K, Schaller M. MAP kinases and cell migration. J Cell Sci 2004;117:4619–28.

25. Reddy K, Nabha S, Atanaskova N. Role of MAP kinase in tumor progression and invasion. Cancer Metastasis Rev 2003;22:395–403.

26. Sebolt-Leopold J, Herrera R. Targeting the mitogen-activated protein kinase cascade to treat cancer. Nat Rev Cancer 2004;4:937–47.

27. Glading A, Bodnar R, Reynolds I, et al. Epidermal growth factor activates m-calpain (calpain II), at least in part, by extracellular signal-regulated kinase-mediated phosphorylation. Mol Cell Biol 2004;24:2499–512.

28. Hunger-Glaser I, Salazar E, Sinnett-Smith J, Rozengurt E. Bombesin, lysophosphatidic acid, and epidermal growth factor rapidly stimulate focal adhesion kinase phosphorylation at Ser-910: requirement for ERK activation. J Biol Chem 2003;278:22631–43.

29. Liu Z, Yu C, Nickel C, Thomas S, Cantley L. Hepatocyte growth factor induces ERK-dependent paxillin phosphorylation and regulates paxillin-focal adhesion kinase association. J Biol Chem 2002;277:10452–8.

30. Seales E, Jurado G, Singhal A, Bellis S. Ras oncogene directs expression of a differentially sialylated, functionally altered β_1 integrin. Oncogene 2003;22:7137–45.

31. Gu J, Zhao Y, Isaji T, et al. β1,4-*N*-Acetylglucosaminyltransferase III down-regulates neurite outgrowth induced by costimulation of epidermal growth factor and integrins through the Ras/ERK signaling pathway in PC12 cells. Glycobiology 2004;14:177–86.

32. Kitada T, Miyoshi E, Noda K, et al. The addition of bisecting *N*-acetylglucosamine residues to E-cadherin down-regulates the tyrosine phosphorylation of β-catenin. J Biol Chem 2001;276:475–80.

33. Huang M, Laskowska A, Vestweber D, Wild M. The α(1,3)-fucosyltransferase Fuc-TIV, but not Fuc-TVII, generates sialyl Lewis X-like epitopes preferentially on glycolipids. J Biol Chem 2002;277:47786–95.